

# UC Irvine

## UC Irvine Previously Published Works

### Title

Strength resistance factors for seismic design of exposed based plate connections in special steel moment resisting frames

### Permalink

<https://escholarship.org/uc/item/9kx4d9wv>

### Journal

Earthquake Spectra, 36(2)

### ISSN

8755-2930

### Authors

Torres-Rodas, Pablo  
Fayaz, Jawad  
Zareian, Farzin

### Publication Date

2020-05-01

### DOI

10.1177/8755293019891714

Peer reviewed

# Strength resistance factors for seismic design of exposed based plate connections in special steel moment resisting frames

Earthquake Spectra

2020, Vol. 36(2) 537–553

© The Author(s) 2020

Article reuse guidelines:

[sagepub.com/journals-permissions](https://sagepub.com/journals-permissions)

DOI: 10.1177/8755293019891714

[journals.sagepub.com/home/eqs](https://journals.sagepub.com/home/eqs)

Pablo Torres-Rodas<sup>1</sup>, Jawad Fayaz, M.EERI<sup>2</sup> and Farzin Zareian, M.EERI<sup>2</sup>

## Abstract

This study presents a critical assessment of the reliability of current base plate connections in steel special moment resisting frames (SMRFs). Using a probabilistic outlook, this research evaluates the reliability of exposed column base (ECB) connections in SMRFs designed based on the current seismic design provisions; it suggests (and implements) a statistical approach to compute resistance factors for three modes of failure (concrete bearing, base plate yielding at tensile interface, and anchor bolt fracture) of ECB connections to achieve a target reliability index,  $\beta$ , of 4.5. Since ECB connections are limited to short buildings, therefore, this study is conducted on two-story and four-story SMRFs which are analyzed using a suite of 120 ground motions originating from strike-slip and reverse faults. ECB connections for the two-story building are designed to simulate pinned connection, while the bases of the four-story building represent moment connections. Detailed methodology for calculating the  $\beta$  of ECB connections is presented considering the three limit states in a moment–axial load interaction curve. Results indicate that the implementation of current seismic provisions results in  $\beta \sim 3.3$  for non-moment resisting ECB connections for all tried combinations of resistance factors. For moment resisting ECB connections, however, only the designs based on a resistance factor for concrete bearing failure mode less than the current 0.65 result in an acceptable reliability factor of  $\beta > 4.5$ .

## Keywords

Exposed column base connections, reliability, SMRF

Date received: 21 December 2018; accepted: 28 August 2019

<sup>1</sup>College of Sciences and Engineering, Universidad San Francisco de Quito, Quito, Ecuador

<sup>2</sup>Department of Civil and Environmental Engineering, University of California, Irvine, Irvine, CA, USA

## Corresponding author:

Farzin Zareian, Department of Civil and Environmental Engineering, University of California, Irvine, Irvine, CA 92697, USA.

Email: [zareian@uci.edu](mailto:zareian@uci.edu)

## Introduction

Column base connections are one of the most important components of steel moment resisting frames (SMRFs). These connections primarily transfer the demands (i.e. axial loads, shear forces and moments) from the superstructure into the substructure (i.e. foundation). In low- to mid-rise SMRF buildings, exposed base plates are typically used to connect the steel columns of the base floor of the building to the foundation system. This configuration comprises several members which include steel column, base plate, anchor rods, grout, and concrete foundation. Figure 1 schematically illustrates this type of connection. In earthquake-resistant systems, exposed base plates are used to transmit moment and axial load demands accompanied by shear forces from the superstructure to the substructure. For gravity systems, however, base plates mainly transfer the axial loads to the foundation.

The response of exposed column base (ECB) connections is controlled by complex interactions of its components which include tensile yielding of base plate or anchor rods, contact gapping between base plate and concrete/grout, interaction of the head nut and top part of the base plate, and friction between base plate and grout. Several studies have been conducted to characterize the strength, stiffness, and deformation capacity of ECB connections. Earlier experimental programs, such as the works by Astaneh et al. (1992), Burda and Itani (1999), Fahmy et al. (1999), contributed to the development of analytical models (e.g. Drake and Elkin, 1999) that suggested design methodologies, such as the Steel Design Guide 1 (Fisher and Kloiber, 2006) which is widely incorporated in the current engineering practice.

Recent experimental programs conducted by Gomez et al. (2010) and Kanvinde et al. (2014) provided new insights of ECB connections behavior resulting in refinements of the

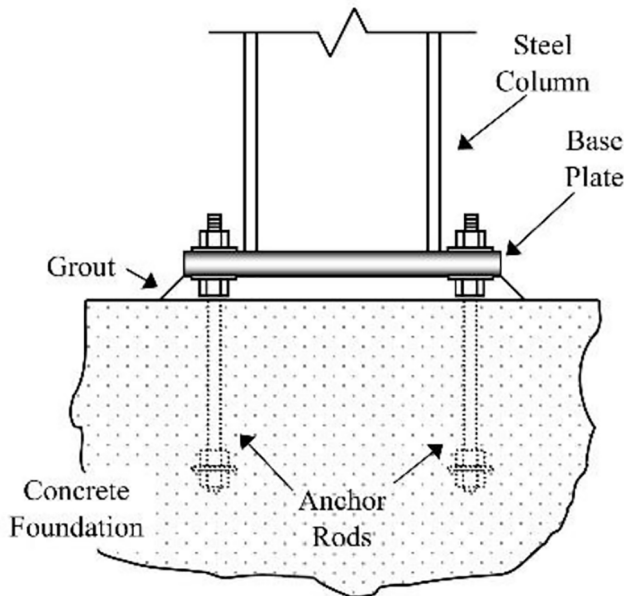


**Figure 1.** Illustration of exposed column base connections.

design methodology described by the Steel Design Guide 1 (Fisher and Kloiber, 2006). Other studies, such as the works by Latour et al. (2014) and Picard and Beaulieu (1985), have addressed rotational flexibility of these connections. Kanvinde et al. (2012) proposed a method to characterize the rotational stiffness of ECB connections by aggregating deformations of its components. This method has been further validated by Trautner et al. (2015) against laboratory test data. Stamatopoulos and Ermopoulos (2011) developed strategies for finite element simulation of ECB connections, while Torres-Rodas et al. (2016) proposed a new hysteretic model to capture the cyclic moment rotation response of ECB connections. The abundance of research in these connections highlights its importance and impact in the performance of SMRFs as indicated by Zareian and Kanvinde (2013). The studies on ECB connections have been synthesized into design guidelines including Seismic Design Manuals from American Institute of Steel Construction (AISC) 341-10 (2010), the Steel Design Guide 1 (Fisher and Kloiber, 2006), and the example detailed in Structural Engineers Association of California (Grilli and Kanvinde, 2013) which constitute the basis of modern design of ECB connections in the United States.

The current design of base plates is based on the Load and Resistance Factor Design (LRFD) methodology which has evolved from American National Standard A58 (ANSI A58 8.1-1980) by Ellingwood et al. (1980). In LRFD methodology, load and resistance factors (i.e. denoted generally with  $\gamma$  and  $\phi$ , respectively) are calibrated to achieve a set Target Reliability (Cornell, 1969). Reliability of a component is defined as the probability of no failure, where failure is said to happen when the component surpasses any of its defined limit states (Ellingwood et al., 1980, 1982). Reliability of a structure is expressed in terms of “Reliability” or “Safety” Index  $M_u = 1.2M_D + 0.5M_L + \Omega_o M_E$ . The values of Target Reliability Index (denoted as  $\beta_T$ ) are set independently for each load combination depending on several factors such as the type of load and material, the expected type of failure (i.e. ductile vs fragile), and the local regulations of the country (i.e. acceptable risk) (Cornell, 1969). These range from  $\beta_T = 1.5$  for some tension members to over  $\beta_T = 7$  for certain masonry walls (Ellingwood et al., 1980). For steel and concrete structures,  $\beta_T = 3$  is set for load combinations including only gravity loads, while  $\beta_T = 2.5$  and  $\beta_T = 1.75$  are selected for load combinations including wind loads and earthquake loads, respectively. The Target Reliability  $\beta_T$  of steel connections for the tensile failure of bolts and flexural failure of plates is set to be 4.5 (i.e. probability of failure within 50-year lifetime  $\approx 3.4 \times 10^{-6}\%$ ).

In the recent reliability study by Aviram et al. (2010) conducted on a base connection belonging to a three-story building located at Berkeley, California, it was observed that the probability of failure of the connections in a 50-year period equals 2.43% (corresponding to a reliability index  $\beta = 1.97$ ) based on a total of seven failure modes (the failure modes analyzed are the ones reported in Steel Design Guide 1). The methodology of analysis employed consisted of establishing a limit state formulation for each failure mode of the base plate. Component and system reliability were conducted using the first-order reliability method (FORM) for four different seismic hazard levels. It was also concluded in this study that the most likely failure modes of the analyzed column base connection were yielding of the base plate on the compression side (ductile), concrete compression crushing (brittle), and shear failure due to base plate sliding and bearing failure of shear lugs (brittle). Furthermore, Iervolino and Galasso (2012) presented the range of  $\beta$  factors corresponding to different values of central safety factor ( $\phi_o$ ) by changing the load ratios between the live and dead loads for various limit states. Also, a recent study by Fayaz and Zareian (2019) presented a detailed probabilistic methodology to assess the reliability of building structures undergoing dead, live, and earthquake loads.

This article explicitly develops a capacity limit state formulation for ECB connections considering the  $M$ - $P$  interaction. Using the suggested limit state formulation, the reliability of the ECB connections of steel special moment resisting frames (SMRF) steel buildings is assessed and modifications are recommended to achieve  $\beta_T$ . The design of the ECB connections used in this study is based on the current seismic criteria of ASCE 7-16 (ASCE, 2016). It aims to build a simplified procedure to assess the probability of failure of the base plate connections. Since exposed base plates are generally used in low-rise structures, the study is conducted on two-story and four-story SMRF buildings which are analyzed under 120 sets of bi-directional ground motions. A series of nonlinear time history analyses conducted on the SMRF buildings form the basis of the demand assessment. Unlike earlier studies (e.g. Aviram et al., 2010), the seismic demands are explicitly treated as random variables and the capacity of the base plates is derived based on  $P$ - $M$  interaction rather than the conventional limit states. Within this framework, the reliability index ( $\beta$ ) of base plates for different design settings is calculated for various combinations of the three resistance factors ( $\phi_{\text{Bearing}}$ ,  $\phi_{\text{Flexure}}$ , and  $\phi_{\text{Fracture}}$ ) and compared with the target reliability index ( $\beta_T$ ). Furthermore, based on the results of these comparisons, suggestions for the current design of base plates are provided.

## Background

Referring to Figure 2, ECB connections resist the imposed load demands of the superstructure (i.e. axial force and bending moment) by developing a force-couple that consists of bearing stresses underneath the base plate in the compression side and axial tensile forces in the anchor rods. This approach (adopted in the Steel Design Guide 1) relies on a predetermined form of stress distribution of the compressive bearing stresses. The stress distribution is simplified to a uniform type (rectangular stress block). As per this assumption, the ECB connections may resist the applied forces (i.e. axial compression and bending moment) through (1) exclusively by bearing stresses under the base plate in the compression zone (i.e. small eccentricity) and (2) by a force-couple created by tensile axial forces in the anchor rods and compression bearing stresses between base plate and the foundation (i.e. large eccentricity). Low eccentricities and large eccentricities are separated through critical eccentricity ( $e_{\text{crit}}$ ) as given in Equation 1 (Drake and Elkin, 1999):

$$e_{\text{crit}} = \frac{N}{2} - \frac{P}{2 \times B \times f_{\text{max}}} \quad (1)$$

$$f_{\text{max}} = 0.85 \times f'_c \times \left( \sqrt{\frac{A_2}{A_1}} \right) \leq 1.7 \times f'_c \quad (2)$$

In Equation 1,  $N$  is the length of the base plate,  $P$  is the compressive axial load,  $B$  is the width of the base plate, and  $f_{\text{max}}$  is the rectangular stress block derived using Equation 2. If the eccentricity (i.e.  $e = M/P$ ) is less than the critical eccentricity (i.e. small eccentricity), the only possible mode of failure is yielding of the base plate in the compression side, resulting from the upward bearing stresses. The magnitude  $f$  and length  $Y$  of the bearing stress are determined by Equations 3 and 4 (Drake and Elkin, 1999):

$$f = \frac{P^2}{P \times B \times N - 2 \times M \times B} \quad (3)$$

$$Y = N - \frac{2 \times M}{P} \quad (4)$$

On the other hand, if the eccentricity ( $e = M/P$ ) is greater than the critical value, then the base plate uplifts from the concrete foundation developing tensile forces in the anchor rods. Three limit states are possible under this scenario: (1) yielding of the base plate in the compression side, (2) yielding of the base plate in the tension side due to downward forces in the anchor rods, and (3) fracture of the anchor rods. The anchor rod forces,  $T$ , as well as the length of the rectangular stress block,  $Y$ , are obtained by equilibrium in the connection using Equations 5 and 6 (Drake and Elkin, 1999):

$$Y = (N - g) - \sqrt{(N - g)^2 - \frac{2 \times [M + P \times (\frac{N}{2} - g)]}{f_{\max} \times B}} \quad (5)$$

$$T = f_{\max} \times B \times \left\{ (N - g) - \sqrt{(N - g)^2 - \frac{2 \times [M + P \times (\frac{N}{2} - g)]}{f_{\max} \times B}} \right\} - P \quad (6)$$

The current design provision associates the design strength of the connection with the first attainment of one of the three above-mentioned limit states, and the corresponding moment is defined as the moment at first yield  $M_y$ . The procedure for calculating the moment at first yield  $M_y$  is briefly described below.

For a given design configuration of column base connection, a predefined stress distribution of bearing stresses (refer to Figure 2) in the compression side of the connection is considered (e.g. rectangular stress block). Internal forces in the component consisting of axial tension in anchor rod and bending moment in the base plate in both compression and tension side are calculated by solving the equilibrium Equations 2, 5, and 6 for a given axial compression force and moment. These internal forces are then compared with the capacities of their corresponding components (i.e. anchor bolts in tension and base plate

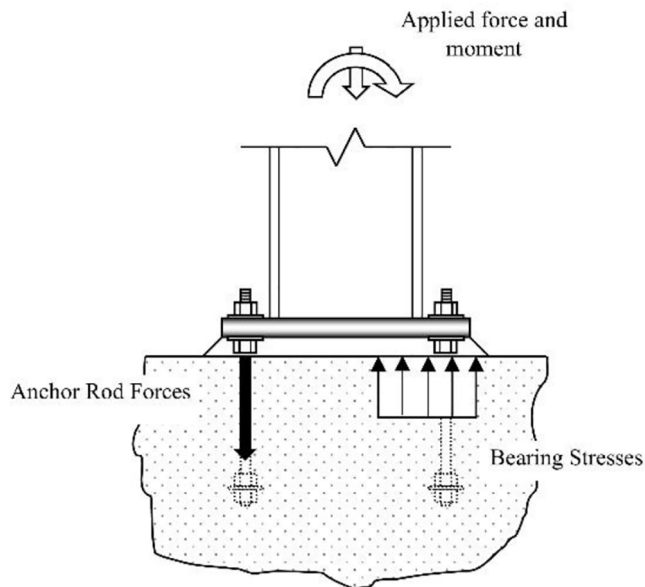


**Figure 2.** Internal forces on exposed column base connections.

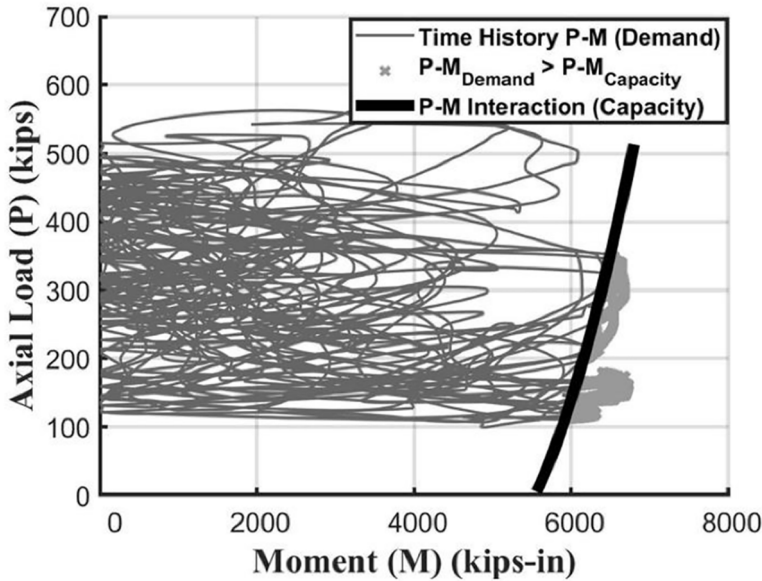


**Figure 3.** *M-P* interaction demand versus capacity curve of ECB connections.

subjected to bending). Keeping the axial force constant, moments in the base plate are incremented until any of its limit states is attained. The corresponding moment is defined as the moment at first yield  $M_y$ .

In this article, limit state of the base plate connection is formulated by computing the moment at first yield  $M_y$  for a vast range of axial compressive forces. This leads to a distinct *M-P* interaction curve (refer to Figure 3) of the capacity of each specific configuration (i.e. base plate size, diameter of bolt, etc.) which is then used to compute the probability of collapse of the ECB connection and hence its correspondent reliability index ( $\beta$ ).

## Models and design of base connections

Base forces (i.e. axial compression and bending moment) for the design of the connection are computed by conducting linear elastic analysis, as specified by code (ASCE 7-16), on both SMRF buildings (i.e. two- and four-story). Dead load of 100 psf (4.78 kN/m<sup>2</sup>) is applied at each floor, and a perimeter load of 25 psf (1.2 kN/m<sup>2</sup>) is applied to represent cladding. In addition, an unreduced live load of 50 psf (2.40 kN/m<sup>2</sup>) is applied at each floor except the roof where live load of 20 psf (0.96 kN/m<sup>2</sup>) is applied. Earthquake loads are calculated by conducting a static pushover using the base shear calculated through the design spectrum shown in Figure 4.

Base connections are designed as pin supports in low-rise buildings (e.g. two-story); for slightly taller buildings (e.g. four-story), however, bases are considered as fixed connections (Zareian and Kanvinde, 2013). Current design guidelines including Seismic Design Provisions (AISC, 2016) and Seismic Design Manual's example 8 (Grilli and Kanvinde, 2013) recommend the use of capacity design principles for the design of ECB connections (i.e. strong connection—weak column) with the intention to protect the connection from

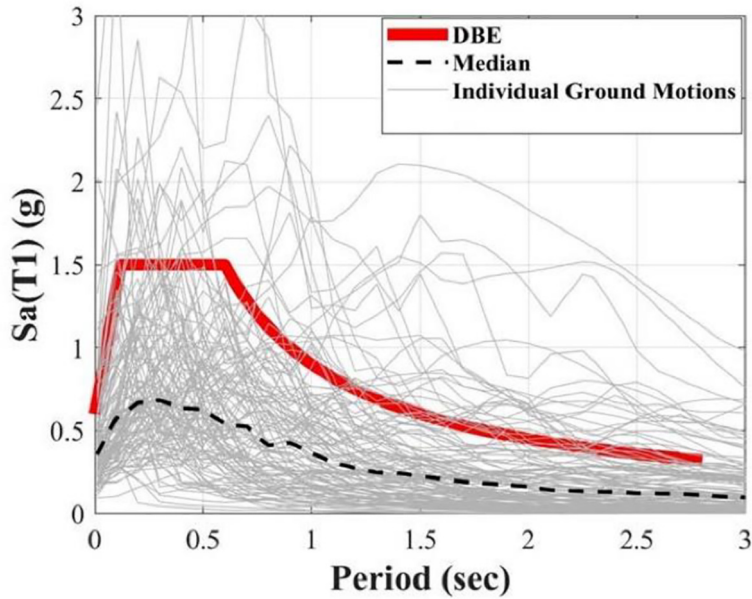


**Figure 4.** Design spectra and response spectra of each ground motion applied.

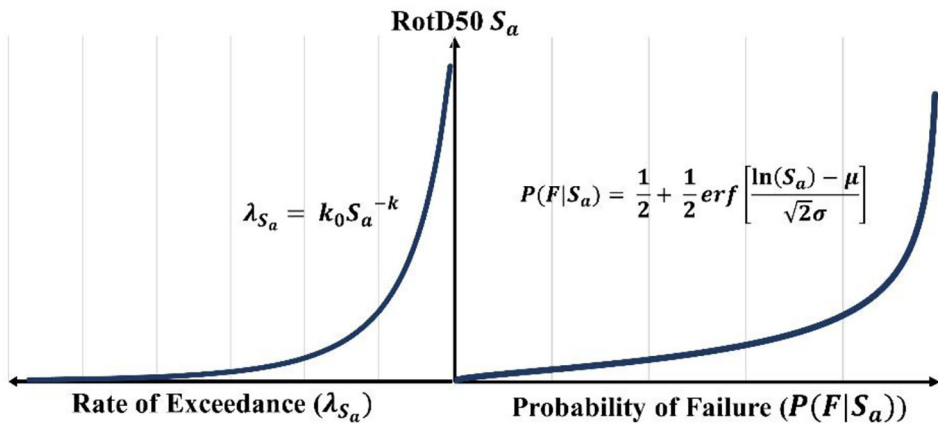


**Figure 5.** IM versus EDP versus lambda IM.

plastic strains. Consequently, two load combinations are considered in this study for each of the two (interior and exterior) ECB connections within each SMRF. The first one deems system overstrength factor,  $\Omega_o$ , to amplify the prescribed seismic design forces (i.e. axial compression and bending moment), whereas the second load combination calculates the forces developed by the ductile members that can be transferred to ECB connection. Hence, for the two-story building, the following two combinations,  $P_u = (1.2 + 0.2S_{DS})P_D + 0.5P_L + \Omega_0P_E$  and  $P_u = (1.2 + 0.2S_{DS})P_D + 0.5P_L + Q$ , are considered in the design of ECB connections, where  $P_D$  corresponds to the axial load due to dead

loads,  $P_L$  corresponds to live load;  $\Omega_o P_E$  is the overstrength seismic load,  $Q$  represents the summation of shear forces in all beams assuming that all the beams fully reached their plastic limit and  $S_{DS}$  is the short-period design value spectral acceleration of the site (American Society of Civil Engineers/Structural Engineering Institute ASCE/SEI 7-06 2006). Since the two-story building is analyzed with pinned bases, therefore, no bending moments are considered in the design. On the other hand, for the four-story building (analyzed with bases simulated as fixed), the two load combinations considered for design are:  $P_u = (1.2 + 0.2S_{DS})P_D + 0.5P_L + \Omega_o P_E$ ,  $M_u = (1.2 + 0.2S_{DS})M_D + 0.5M_L + \Omega_o M_E$  and  $P_u = (1.2 + 0.2S_{DS})P_D + 0.5P_L + Q$ ,  $M_u = 1.1R_y M_p$ . The subscripts  $D$ ,  $L$ , and  $E$  represent the moments and axial loads due to dead load, live load, and earthquake forces, respectively, and  $M_p$  represents the plastic moment of the attached column. The resistance factors considered in these designs are as follows: (1) resistance factor for bending— $\phi_b$ , (2) resistance factor for bearing— $\phi_c$ , and (3) resistance factor for fracture— $\phi_f$ . Each of these resistance factors is associated with its corresponding limit state of the ECB connection (i.e. bending of the base plate, fracture of the anchor rods, and concrete crushing). According to the Steel Design Guide 1 (Fisher and Kloiber, 2006), the recommended values of these resistance factors are  $\phi_b = 0.9$ ,  $\phi_c = 0.65$ ,  $\phi_f = 0.75$ . Thus, a set of resistance factors which lead to different ECB configurations (refer to Tables 1 to 3) are regarded in this article to assess their reliability and find the appropriate set that matches target reliability index.

As described in previous section, two steel SMRFs varying in height are considered in this research (i.e. two- and four-story). Since this study is limited to the exposed base plates, only low-rise and mid-rise buildings are considered for the reliability analysis. The building frames consist of three bays (6 m each), with heights ranging from 8.5 m (two-story) to 16.5 m (four-story). The buildings are derived from the ATC-72 project; for further details, refer to National Institute of Standards Technology (NIST, 2010). The buildings are designed as per ASCE 7-05 (2006), the connections are detailed as reduced beam section (RBS) following the Seismic Provisions AISC 341-10 (2010) with  $R = 8$ , and site class D conditions under the seismic design category  $D_{max}$ . The fundamental periods of the two- and four-story SRMFs are 0.56 and 0.95 s, respectively. Open-source software OpenSees (McKenna et al., 2000) is used for the nonlinear dynamic simulations.

**Table 1.** Reliability indexes ( $\beta$ ) for two-story building with  $\phi_f = 0.75$ .

Exterior column						
$\phi_b$	$\phi_c$					
	0.45	0.55	0.65	0.75	0.85	0.95
0.50	3.32	3.35	3.34	3.34	3.35	3.35
0.60	3.32	3.35	3.34	3.34	3.35	3.35
0.70	3.32	3.35	3.34	3.34	3.35	3.35
0.80	3.32	3.35	3.34	3.34	3.35	3.35
0.90	3.32	3.35	3.34	3.34	3.35	3.35
1.00	3.32	3.35	3.34	3.34	3.35	3.35
Interior column						
0.50	3.68	3.70	3.70	3.70	3.70	3.70
0.60	3.68	3.70	3.70	3.70	3.70	3.70
0.70	3.68	3.70	3.70	3.70	3.70	3.70
0.80	3.68	3.70	3.70	3.70	3.70	3.70
0.90	3.68	3.70	3.70	3.70	3.70	3.70
1.00	3.68	3.70	3.70	3.70	3.70	3.70

**Table 2.** Reliability indexes ( $\beta$ ) for four-story building corresponding to case  $P_u = 1.2P_D + 0.5P_L + \Omega_0 P_E$ ;  $M_u = 1.2M_D + 0.5M_L + \Omega_0 M_E$  with  $\phi_f = 0.75$ .

Exterior column						
$\phi_b$	$\phi_c$					
	0.45	0.55	0.65	0.75	0.85	0.95
0.50	5.00	5.00	5.00	3.05	0.28	0.28
0.60	5.00	5.00	5.00	3.05	0.28	0.28
0.70	5.00	5.00	5.00	3.05	0.28	0.28
0.80	5.00	5.00	5.00	3.05	0.28	0.28
0.90	5.00	5.00	5.00	3.05	0.28	0.28
1.00	5.00	5.00	5.00	3.05	0.28	0.28
Interior column						
0.50	5.00	5.00	5.00	3.00	3.00	0.43
0.60	5.00	5.00	5.00	3.00	3.00	0.43
0.70	5.00	5.00	5.00	3.00	3.00	0.43
0.80	5.00	5.00	5.00	3.00	3.00	0.43
0.90	5.00	5.00	5.00	3.00	3.00	0.43
1.00	5.00	5.00	5.00	3.00	0.46	0.43

**Table 3.** Reliability indexes ( $\beta$ ) for four-story building corresponding to case  $P_u = 1.2P_D + 0.5P_L + Q$ ;  $M_u = 1.1R_y M_p$  with  $\phi_f = 0.75$ .

Exterior column						
$\phi_b$	$\phi_c$					
	0.45	0.55	0.65	0.75	0.85	0.95
0.50	2.10	5.00	1.26	3.05	3.05	0.28
0.60	2.10	5.00	1.26	3.05	3.05	0.28
0.70	2.10	5.00	1.26	3.05	3.05	0.28
0.80	2.10	5.00	1.26	3.05	3.05	0.28
0.90	2.10	5.00	1.26	3.05	3.05	0.28
1.00	1.05	0.78	1.26	3.05	-0.1	-0.1
Interior column						
0.50	2.52	2.95	2.95	0.43	0.43	0.43
0.60	2.52	2.95	2.95	0.43	0.43	0.43
0.70	2.52	2.95	2.95	0.43	0.43	0.43
0.80	2.52	2.95	2.95	0.43	0.43	0.43
0.90	0.55	0.51	2.95	0.43	0.43	0.43
1.00	0.55	0.51	0.47	0.43	0.43	-1.0

The SMRFs systems are modeled as two-dimensional (2D) plane frames with the beams and columns provided as elastic elements with concentrated plasticity at their ends (and at RBS location in the case of beams). The hysteretic response of the plastic hinges is represented through Ibarra–Medina–Krawinkler (IMK) bilinear model developed by Ibarra et al. (2005) and modified by Lignos and Krawinkler (2011). This hysteretic model has a trilinear backbone curve and appropriate rules to capture strength and stiffness cyclic deterioration. The parameters for the backbone and the hysteresis are calibrated from a compilation of 300 component tests assembled by Lignos and Krawinkler (2011). These

springs inherit the limitations of uniaxial concentrated plasticity model. Consequently, they cannot directly simulate axial force–moment interactions in the columns. This problem is addressed in an approximate manner. First, average axial loads in columns are obtained from combined actions of gravity and lateral loading by performing a gravity and nonlinear pushover static analysis. Then, the moment strength of column hysteretic backbone curve is reduced using beam–column interaction equations (AISC, 2011) using an axial load estimated as  $P_{gravity} + 0.5 \times P_{\Omega_0 E}$  where  $P_{gravity}$  represents the axial load coming from gravity loads (i.e.  $(1.2 + 0.2S_{DS})P_D + 0.25P_L$ ) and  $P_{\Omega_0 E}$  the amplified axial load due to seismic effects. The panel zones are modeled as a parallelogram with a nonlinear model simulated by a spring at one corner. The properties of these hysteretic models are calculated as per Applied Technology Council (ATC, 2010). A leaning column is used to induce  $P - \Delta$  effects in conjunction with a large deformation transformation (i.e.  $P - \Delta$  transformation) to simulate side-sway collapse. Rayleigh damping of 2.5% is assigned at the first mode period  $T_1$  and at  $T = 0.2T_1$ .

Other studies have shown that the rotational flexibility of exposed base connections has significant impact on the performance of SMRFs (Zareian and Kanvinde, 2013) and, consequently, on the force and moment demands. Thus, in this article, the rotational stiffness is calculated following the methodology developed by Kanvinde et al. (2012) and validated by Trautner et al. (2015). This method estimates base flexibility of ECB connections by aggregating deformations within the components of the connection (i.e. base plate, anchor rods and concrete foundation). ECB connections are modeled as a linear elastic spring. This criterion is consistent with current Seismic Design Provisions (AISC 341-10, 2010) that promote yielding in the column itself rather than the base connection. (i.e. capacity design criteria).

## Ground motions

The demands on ECB connections are estimated through detailed nonlinear dynamic simulations. The models described above are subjected to a suite of 120 ground motions with  $M_w > 6.5$ , which are obtained from NGAWest2 (Timothy et al., 2014) database. The suite of 120 ground motions consists of 4 sets of 30 records originating from different source conditions. These include the following: (1) near-fault ( $R_{rup} < 15$  km) ground motions originating from reverse fault mechanism, (2) near-fault ( $R_{rup} < 15$  km) ground motions arising from strike-slip mechanism, (3) far-fault ( $R_{rup} > 15$  km) ground motions originating from reverse fault mechanism, and (4) far-fault ( $R_{rup} > 15$  km) ground motions deducing from strike-slip mechanism. This resulting suite of 120 ground motions is scaled to match eight different hazard levels described in Table 4. Referring to Table 4, three of the eight hazard levels represent the frequent earthquake (i.e. average recurrence interval of 72 years), design basis earthquake (i.e. average recurrence interval of 475 years), and maximum considered earthquake level (i.e. average recurrence interval of 2475). These earthquake design levels are associated with their corresponding performance limits of immediate occupancy, life safety, and collapse prevention, respectively. The remaining levels supplement the results from the time history simulations to build up an appropriate representation of fragility curves for the reliability analysis.

## Reliability assessment methodology

The reliability assessment of each designed ECB connection is accomplished by following four steps.

### Step 1: Assessing the strength of the connection

Referring to the introductory section, the strength of the ECB connection is associated with the first attainment of one of the limit states defined by (1) flexural yielding of the base plate in the compression side due to bearing stresses, (2) yielding of the base plate in the tension side of the connection due to axial tensile forces in the anchor rods, and (3) fracture of the anchor rods. The first two limit states capacities are determined as per Equation 7, while the latter is defined by Equation 8. In these equations,  $F_y$  is the yield strength of the base plate;  $B$ ,  $t_p$  are the width and thickness of the base plate, respectively;  $F_{u,rod}$  is the tensile strength of the anchor rod; and  $A_n$  is the total tensile area of anchor rods in tension. The applied moment corresponding to the *first yield* of any component (i.e.  $M_y$ ) defines the strength of the ECB connection, for a specific configuration (size, thickness, etc.) and level of axial load. Thus, the moment at first yield  $M_y$  is calculated for a vast range of axial loads which results in a formulation of limit state of the ECB connection:

$$M_{plate}^{base} = F_y \times B \times \frac{t_p^2}{4} \quad (7)$$

$$T_{rod} = 0.75 \times F_{u,rod} \times A_n \quad (8)$$

Other limit states on ECB connections such as concrete crushing, shear failure, pull-out failure of anchor bolts, concrete breakout of anchor bolts, and weld fracture have been reported in the past (e.g. Astaneh et al., 1992; Gomez et al., 2010; Aviram et al., 2010). However, in this study, these limit states are not considered in the reliability analysis since they are unlikely to happen as their strengths are deduced to be significantly higher than their corresponding demands which results in high safety factors. Specifically, (1) the size of the base plate is defined by the dimensions of the column and Occupational Safety and Health Administration (OSHA) recommendations for constructability rather than by attainment of the maximum stresses in the concrete, consequently, no concrete crushing is expected in this study; (2) shear demands are held only by friction between the base plate and grout; (3) pull-out failure of anchor rods and concrete breakout may be prevented with an appropriate detailing of the connection including sufficient concrete area and reinforcement of the pedestal; and (4) current weld details prevent fracture until large deformations (0.8 rad) which imply that the connection would fail before these levels of deformation are achieved.

### Step 2: Assessing the demands on the connection

The scientific basis to obtain the seismic demands is by conducting a series of nonlinear time history analysis of SMRF models under various seismic hazard levels (refer to Table 4). As the influence of base flexibility in these simulations is appropriately considered, they represent an accurate estimate of the demands in the ECB connection. For each simulation, Engineering Demand Parameter (EDP) histories of bending moment, axial forces, and shear forces are recorded. While the shear force demands are considered negligible in base connections (Gomez et al., 2010), interaction of axial force and moment demands is compared with the capacity  $M$ - $P$  limit state formulated for the ECB connections. ECB connections are controlled by  $M$ - $P$  interactions rather than a peak flexural moment or peak axial load (Torres-Rodas et al., 2018). This  $M$ - $P$  interaction limit state is developed as explained in *step 1*.

**Table 4.** Hazard levels.

Case	Prob. exc.	$\Lambda^a$	Return period
1	0.72	0.0255	39
2 <sup>b</sup>	0.5	0.0139	72
3	0.42	0.0109	92
4	0.28	0.0066	152
5 <sup>b</sup>	0.1	0.0021	475
6	0.05	0.0010	975
7	0.03	0.0006	1642
8 <sup>b</sup>	0.02	0.0004	2475

<sup>a</sup>Mean annual rate of exceedance.

<sup>b</sup>I.O., D.E., M.C.E.

### Step 3: Estimation of probability of failure

The demands on ECB connections are obtained by applying the 120 ground motions on the suggested building models and conducting nonlinear analysis. The demands are then compared with the formulated capacity  $M-P$  interaction curve from which probability of failure conditioned on intensity measure of the corresponding return period  $P(F|S_a)$  is estimated. Elaborating on this, for a given return period, all the ground motions are scaled to achieve corresponding  $S_a$ , and for each ground motion, the  $M-P$  interaction of demand and capacity is compared. Base plate connection is said to fail under a ground motion if any point in the  $M-P$  interaction time history exceeds the formulated capacity  $M-P$  interaction curve, as exhibited in Figure 3. Probability of failure is calculated using Equation 9 by employing this approach for each ground motion at a given hazard:

$$P(F|S_a) = \frac{\text{Number of ground motions causing failure}}{\text{Total number of ground motions}(=120)} \quad (9)$$

This process is repeated for ground motions scaled to eight different hazard levels provided in Table 4. As per FEMA P695 (2009), probability of failure due to seismic demands and the ground motion intensity measure follows a lognormal distribution. As shown in the right side of Figure 5, the statistical parameters ( $\mu$  and  $\sigma$ ) of the lognormal distribution curve are estimated by fitting a lognormal curve to correlate probability of failure due to seismic demands and the ground motion intensity measure, that is,  $S_a$ , as given in Equation 10:

$$P(F|S_a) = \Phi\left(\frac{\ln S_a - \mu}{\sigma}\right) = 0.5 + 0.5 \operatorname{erf}\left[\frac{\ln S_a - \mu}{\sqrt{2}\sigma}\right] \quad (10)$$

Spectral acceleration hazard curve in the form of probability of exceedance ( $G_{S_a}(S_a)$ ) is obtained using OpenSHA (or any other probabilistic hazard analysis software). Using Poisson's model with period of interest (i.e. life span, denoted as  $t$ ) as 50 years and the procured probability of exceedance ( $G_{S_a}(S_a)$ ), annual rate of exceedance ( $\lambda_{S_a}$ ) is acquired using Equation 10. Hazard levels in the proximity of limit state probability ( $S_a$  with average return period between 25 and 2500 years) can be represented in the form Equation 11 (Jalayer, 2003). By fitting a power curve on the obtained spectral acceleration hazard, parameters  $k_0$  and  $k$  are estimated as shown in the left side of Figure 5:

$$G_{S_a}(S_a) = P[S_a \geq s_a] = 1 - \exp(-\lambda_{s_a} t) \quad (11)$$

$$\lambda_{s_a} = k_o S_a^{-k} \quad (12)$$

The rate of failure (denoted as  $\lambda_F$ ) of a base plate can then be estimated by integrating the  $P(F|S_a)$  over the hazard curve, as given in Equation 13. Probability of failure is calculated using Poisson's equation given in Equation 14. Finally, the reliability index ( $\beta$ ) of the base plate connection is obtained using Equation 15. In this procedure, it is assumed that the capacity of the connection and the demands are statistically independent. Although more accurate methods of approximating the hazard curve and performing closed-form integral of Equation 12 are available (Vamvatsikos, 2012), for the sake of brevity, the authors have limited the computation to the method described above. Finally, the integration of Equation 13 is performed in a discretized manner which is assumed to represent the entire curve:

$$\lambda_F = \int P(F \geq f | S_a = s_a) |d\lambda(s_a)| \quad (13)$$

$$P(F) = \exp(-\lambda_F t) \quad (14)$$

$$\beta = \Phi^{-1}[P(F)] \quad (15)$$

The aforementioned four step procedure is exercised for both interior and exterior column base plate connections of both two-story and four-story buildings for both design combinations which include (1) the system overstrength factor  $(1.2 + 0.2S_{DS})D + 0.5L + \Omega_0 E$  and (2) using plastic capacity of column  $1.1R_y M_p$ .

## Results and discussion

### Two-story building

As discussed above, the ECB connections (for exterior and interior columns) of the two-story building are designed as pinned bases. (i.e. designed only for axial compressive load and zero moment). Two load combinations are considered for the design of ECB connection: (1) including the system overstrength factor,  $\Omega_o$ , and (2) by calculating the forces developed by the ductile members that are transferred to the ECB connection. Moreover, a set of resistance factors are considered (refer to Tables 1 to 3) resulting in two sets (for each load combination) of 36 design configurations. The results of the analysis indicate that the reliability index  $\beta$  for both exterior and interior columns for all the designs ranges from 3.32 to 3.71 (probability of failure ranging from 0.045% to 0.01%). The target reliability index  $\beta_T$  is 4.5 (probability of failure  $\approx 3.4 \times 10^{-6}\%$ ). As shown in Tables 1 to 3, in this study, different combinations of  $\phi$ -factors for limit states of flexure and fracture are used in order to achieve  $\beta_T$ ; however, the results indicate neither the current resistance factors nor any other combinations of the factors result in achievement of the target reliability  $\beta_T = 4.50$  in case of two-story buildings. This may be attributed to the actual stiffness proportioned by the ECB connection (and considered in the nonlinear dynamic simulations). The results undermine the current seismic design provisions of ECB connections in short buildings and, consequently, it is recommended that ECB connections shall not be designed only for axial compressive loads. It is suggested that rotational stiffness must be appropriately estimated (e.g. Kanvinde et al., 2012) and moments should be added in the analysis to obtain more appropriate designs. This observation is consistent with the

findings presented by Torres-Rodas et al. (2018) in a study on seismic demands on column base connections. Moreover, Torres-Rodas et al. (2018) demonstrated that the “capacity/demand” ratio of ECB connections designed as pinned base is quite sensitive to rotational stiffness. This finding highlights the importance of an accurate estimate of the stiffness of the connection.

### Four-story building

Similar to the analysis of two-story building, in four-story building, two load combinations include the system overstrength factor and capacity design principles with different combinations of resistance factors (as shown in Tables 1 to 3). Contrary to the two-story building, the ECB connections for the four-story building are designed considering fixed bases (i.e. for axial compressive force and bending moment). Results of the analysis show that for the first load combination (i.e.  $P_u = (1.2 + 0.2S_{DS})P_D + 0.5P_L + \Omega_0P_E$ ,  $M_u = (1.2 + 0.2S_{DS})M_D + 0.5M_L + \Omega_0M_E$ ), only the designs based on a resistance factor for bearing  $\phi_c \leq 0.65$  result in obtaining  $\beta > 4.5$  (probability of failure  $< \approx 3.4 \times 10^{-6}\%$ ). A closer inspection of the results reveals that this resistance factor for bearing  $\phi_c$  has the most dominant influence on the reliability index  $\beta$  with  $\beta$  increasing as  $\phi_c$  decreases. This is ascribed to the impact that  $\phi_c$  has in the computation of the intensity of the bearing stresses on the compression side of the connection and consequently on the demands on the components of the connection. This trend is observed in both exterior and interior columns of the four-story building. A general observation is that all resulting designs from the second load combination (i.e.  $P_u = (1.2 + 0.2S_{DS})P_D + 0.5P_L + Q$ ,  $M_u = 1.1R_yM_p$ ) lead to lesser  $\beta$ , hence higher probability of failure, than the designs based on the first load combination.

Results also show that for internal columns, all design combinations of resistance factors lead to a  $\beta < 4.5$ , while for the exterior columns, only the designs corresponding to a  $\phi_c = 0.55$  result in  $\beta > 4.5$ . This can be explained by a closer examination of the evolution of  $M - P$  demands in the time history of the simulations. It is noticed that the most critical  $M - P$  demand occurs at the maximum moment accompanied by the minimum (instead of maximum) axial compressive load which is further explained by the shape of the limit state formulation (refer to Figure 3). This indicates an increase in moment capacity with an increase in the axial forces. This observation is also reported in the work by Torres-Rodas et al. (2018) and is related to the physics of ECB connections where the axial compressive forces delay base plate uplift on the tension side of the connection and subsequent limit states (i.e. bending of the base plate in the tension side and anchor rod fracture). Refer to the work by Torres-Rodas et al. (2016) for further details.

### Summary and conclusion

In lieu of earlier research, it is noticed that no substantial investigation has been conducted on the reliability of the ECB connections while incorporating the random nature of the earthquake load for individual buildings. This article examines the reliability of ECB connections undergoing earthquake loads, taking into consideration the actual strength interaction curve of the base plates rather than the conventional conservative approach of taking maximum axial and moment capacities.

The study shows that the failure of ECB connections is associated with the combination of the minimum axial compressive force and the maximum bending moment. This is due

to the compensating effect of axial compressive forces that delay base plate uplift in the tension side of the connection and delaying the flexural bending and anchor rod fracture failure modes. Therefore, the appropriate load combination for design of moment resisting ECB connections must include an estimate of the minimum axial load and highest moment (i.e.  $P_u = (1.2 + 0.2S_{DS})P_D + 0.5P_L - Q$ ;  $M_u = 1.1R_yM_p$ ). Current load combinations employed for design of ECB connections (see Grilli and Kanvinde, 2013) include an estimate of maximum response based on amplification of earthquake forces by the system overstrength factor and capacity design principles (i.e.  $P_u = (1.2 + 0.2S_{DS})P_D + 0.5P_L + \Omega_0P_E$ ;  $M_u = 1.1R_yM_p$ ). The results of this article indicate that for the four-story building when ECB connections are designed with  $P_u = (1.2 + 0.2S_{DS})P_D + 0.5P_L + \Omega_0P_E$  and  $M_u = (1.2 + 0.2S_{DS})M_D + 0.5M_L + \Omega_0M_E$ , and resistance factors recommended by AISC Guide 1 (Fisher and Kloiber, 2006, i.e.  $\phi_b = 0.9$ ,  $\phi_c = 0.65$ , and  $\phi_f = 0.75$ ), the designs are adequate with  $\beta > 4.5$ . When the base plates are sized with capacity design principles, only values of  $\phi_c < 0.65$  lead to  $\beta > 4.5$ .

For the two-story building, however, both load combinations (i.e.  $P_u = (1.2 + 0.2S_{DS})P_D + 0.5P_L + \Omega_0P_E$  and  $P_u = (1.2 + 0.2S_{DS})P_D + 0.5P_L + Q$ ) result in designs which have reliability indices less than 4.5 for all tried load combinations for resistance factors. Based on these results, it is recommended that these ECB connections not be designed solely for axial compressive force. Proper design should include a bending moment estimated based on the rotational stiffness of the connection (for such calculations, see Kanvinde et al., 2012). Furthermore, it is concluded that the current resistance factors involved in the design process of the ECB connections can be altered to achieve more reliable designs.

Irrespective of the above-mentioned results, some limitations can be propelled to this study which must be considered in the implementation of the results. First, only two buildings with different height but same plan configuration are investigated. Other possible configurations may lead to dissimilar results, especially in the case when a corner column is shared between two orthogonal lateral load-resisting systems. Second, including the effect of the vertical component of ground motions, variability in gravity loads, and uncertainty in material strength may alter the estimated  $\beta$  for ECB connections. Third, the response of the models can be sensitive to assumptions such as concentrated versus distributed plasticity models or consideration of soil structure interaction in building seismic response assessment. These limitations can be incorporated in future research so as to obtain more general results of the behavior of ECB connections.

### Declaration of conflicting interests

The author(s) declared no potential conflicts of interest with respect to the research, authorship, and/or publication of this article.

### Funding

The author(s) received no financial support for the research, authorship, and/or publication of this article.

### References

- AISC 341-10 (2010) Seismic provisions for structural steel buildings.
- American Institute of Steel Construction (AISC) (2011) *Steel Construction Manual*. 14th ed. Chicago, IL: AISC.

- American Society of Civil Engineers/Structural Engineering Institute (ASCE/SEI) (2006) *Minimum Design Loads for Buildings and Other Structures*. Reston, VA: ASCE/SEI 7–05.
- American Society of Civil Engineers (ASCE) (2016) *Minimum Design Loads for Buildings and Other Structures*. Reston, VA: ASCE.
- Applied Technology Council (ATC) (2010) *ATC 72–1: Modeling and Acceptance Criteria for Seismic Design and Analysis of Tall Buildings*. Redwood City, CA: ATC.
- Astaneh A, Bergsma G and Shen JH (1992) Behavior and design of base plates for gravity, wind and seismic loads. In: *Proceedings of the national steel construction conference*, Las Vegas, NV, 3–5 June. Chicago, IL: AISC.
- Aviram A, Stojadinovic B and Der Kiureghian A (2010) *Performance and Reliability of Exposed Column Base Plate Connections for Steel Moment-Resisting Frames* (PEER report 2010/107). Berkeley, CA: Pacific Earthquake Engineering Research Center.
- Burda JJ and Itani AM (1999) *Studies of Seismic Behavior of Steel Base Plates* (Report No. CCEER 99-7). Reno, NV: Center of Civil Engineers Earthquake Research, Department of Civil and Environmental Engineering, University of Nevada.
- Cornell A (1969) A probabilistic-based structural code. *ACI Structural Journal* 66(12): 974–985.
- Drake R and Elkin S (1999) Beam-column base plate design LRFD method. *Engineering Journal* 36: 29–38.
- Ellingwood B, Galambos T, MacGregor J, et al. (1980) *Development of a Probabilistic Based Load Criterion for American National Standard A58*. Gaithersburg, MD: National Bureau of Standards.
- Ellingwood B, MacGregor J, Galambos T, et al. (1982) Probability-based load criteria: Load factors and load combinations. *Journal of the Structural Division* 108(5): 978–997.
- Fahmy M, Stojadinovic B and Goel SC (1999) Analytical and experimental studies on the seismic response of steel column bases. In: *Proceedings of the 8th Canadian conference on earthquake engineering*, Vancouver, BC, Canada, 13–16 June.
- Fayaz J and Zareian F (2019) Reliability analysis of steel SMRF and SCBF structures considering the vertical component of near-fault ground motions. *Journal of Structural Engineering* 145(7): 04019061.
- FEMA P695 (2009) Quantification of building seismic performance factors.
- Fisher JM and Kloiber LA (2006) *Steel Design Guide 1—Base Plate and Anchor Rod Design* (AISC 801-06). 2nd ed. Chicago, IL: American Institute of Steel Construction.
- Gomez IR, Kanvinde AM and Deierlein GG (2010) *Exposed Column Base Connections Subjected to Axial Compression and Flexure* (Report). Chicago, IL: American Institute of Steel Construction.
- Grilli DA and Kanvinde AM (2013) Special moment frame base connection: Design example 8. In: *2012 IBC SEAOC Structural/Seismic Design Manual, Examples for Steel-Frame Buildings*, vol. 4, pp. 255–280. Oakland: ICC/SEAOC (International Code Council/Structural Engineers Association of California).
- Ibarra LF, Medina RA and Krawinkler H (2005) Hysteretic models that incorporate strength and stiffness deterioration. *Earthquake Engineering and Structural Dynamics* 34: 1489–1511.
- Iervolino I and Galasso C (2012) Comparative assessment of load-resistance factor design for FRP-reinforced cross sections. *Construction & Building Materials* 34: 151–161.
- Jalayer F (2003) Direct probabilistic seismic analysis: Implementing non-linear dynamic assessments. PhD Dissertation, Stanford University, Stanford, CA.
- Kanvinde AM, Grilli DA and Zareian F (2012) Rotational stiffness of exposed column base connections: Experiments and analytical models. *Journal of Structural Engineering* 138(5): 549–560.
- Kanvinde AM, Higgins P, Cooke RJ, et al. (2014) Column base connections for hollow steel sections: Seismic performance and strength models. *Journal of Structural Engineering* 141(7): 04014171.
- Latour M, Piluso V and Rizzano G (2014) Rotational behaviour of column base plate connections: Experimental analysis and modelling. *Engineering Structures* 68: 14–23.

- Lignos DG and Krawinkler H (2011) Deterioration modeling of steel components in support of collapse prediction of steel moment frames under earthquake loading, *Journal of Structural Engineering* 137: 1291–1302.
- McKenna F, Fenves GL and Scott MH (2000) *Open System for Earthquake Engineering Simulation*. Berkeley, CA: University of California.
- National Institute of Standards Technology (NIST) (2010) *Evaluation of the FEMA P695 Methodology for Quantification of Building Seismic Performance Factors*. Gaithersburg, MD: FEMA.
- Picard A and Beaulieu D (1985) Behaviour of a simple column base connection. *Canadian Journal of Civil Engineering* 12(1): 126–136.
- Stamatopoulos GN and Ermopoulos JCh (2011) Experimental and analytical investigation of steel column bases. *Journal of Constructional Steel Research* 67(9): 1341–1357.
- Timothy DA, Robert BD, Jonathan PS, et al. (2014) NGA-West2 database. *Earthquake Spectra* 30(3): 989–1005.
- Torres-Rodas P, Zareian F and Kanvinde A (2016) A hysteretic model for exposed column base connections. *Journal of Structural Engineering* 142(12): 04016137.
- Torres-Rodas P, Zareian F and Kanvinde A (2018) Seismic demands in column base connections of steel moment frames. *Earthquake Spectra* 34(3): 1383–1403.
- Trautner CA, Hutchinson T, Grosser P, et al. (2015) Effects of detailing on the cyclic behavior of steel base plate connections designed to promote anchor yielding. *Journal of Structural Engineering* 142(2): 04015117.
- Vamvatsikos D (2012) Derivation of new SAC/FEMA performance evaluation solutions with second-order hazard approximation. *Earthquake Engineering and Structural Dynamics* 42(8): 1171–1188.
- Zareian F and Kanvinde A (2013) Effect of column base flexibility on the seismic response and safety of steel moment resisting frames. *Earthquake Spectra* 29(4): 1537–1559.